Water in Channel-Like Cavities: Structure and Dynamics

M. S. P. Sansom, I. D. Kerr, J. Breed, and R. Sankararamakrishnan
Laboratory of Molecular Biophysics, University of Oxford, Oxford OX1 3QU, United Kingdom

ABSTRACT Ion channels contain narrow columns of water molecules. It is of interest to compare the structure and dynamics of such intrapore water with those of the bulk solvent. Molecular dynamics simulations of modified TIP3P water molecules confined within channel-like cavities have been performed and the orientation and dynamics of the water molecules analyzed. Channels were modeled as cylindrical cavities with lengths ranging from 15 to 60 Å and radii from 3 to 12 Å. At the end of the molecular dynamics simulations water molecules were observed to be ordered into approximately concentric cylindrical shells. The waters of the outermost shell were oriented such that their dipoles were on average perpendicular to the normal of the wall of the cavity. Water dynamics were analyzed in terms of self-diffusion coefficients and rotational reorientation rates. For cavities of radii 3 and 6 Å, water mobility was reduced relative to that of simulated bulk water. For 9- and 12-Å radii confined water molecules exhibited mobilities comparable with that of the bulk solvent. If water molecules were confined within an hourglass-shaped cavity (with a central radius of 3 Å increasing to 12 Å at either end) a gradient of water mobility was observed along the cavity axis. Thus, water within simple models of transbilayer channels exhibits perturbations of structure and dynamics relative to bulk water. In particular the reduction of rotational reorientation rate is expected to alter the local dielectric constant within a transbilayer pore.

INTRODUCTION

Transbilayer pores are present in several classes of membrane transport proteins: ion channels (Unwin, 1989; Hille, 1992), bacterial porins (Cowan et al., 1992), and aquaporins (Engel et al., 1994). In all these proteins water molecules may be found within the lumen of the pore (Kreusch and Schulz, 1994; Unwin, 1995). Evidently the physical properties of intrapore water play an important role in governing the transport properties of the pore (Dani and Levitt, 1990; Karshikoff et al., 1994). For example, the dynamic behavior of intrapore water will influence the local dielectric constant and hence the electrostatic field within the pore. There have been numerous studies, both experimental and computational (Teeter, 1991; Daggett and Levitt, 1993), of the properties of water molecules interacting with the surface of globular proteins. Somewhat less is known of the structure and dynamics of water molecules inside transbilayer channels (Chiu et al., 1991, 1993; Green and Lu, 1995; Sancho et al., 1995). A first step to characterizing the properties of such systems is to examine how water molecules behave when they are confined in channel-like cavities.

There is considerable evidence that liquids confined within volumes of molecular dimensions differ in their properties from the same solvent in its "bulk" state (Granick, 1991). In particular, a number of studies have employed molecular dynamics (MD) to simulate the behavior of water molecules located between two planar hydrophobic surfaces (Jonsson, 1981; Marchesi, 1983; Barabino et al., 1984; Lee et al., 1984; Rossky and Lee, 1989) or within spherical hydrophobic pockets (Belch and Berkowitz, 1985; Zhang et al., 1995). Such studies indicate that water confined in such environments exhibits a greater degree of order than in the bulk solvent, with the formation of distinct "layers" of molecules parallel to the surface. Furthermore, the dynamic properties of the water close to the surface are perturbed, although there is some disagreement concerning the extent of such perturbations (Marchesi, 1983; Barabino et al., 1984; Zhang et al., 1995).

In this study we use MD simulations to investigate the structure and dynamics of water molecules confined within channel-like cavities. Two cavity geometries are considered: cylindrical and "hourglass-shaped." The dependence of the water behavior on the shape and dimensions of the cavity is investigated. The results indicate that ordering and immobilization of water occurs within these channel-like cavities. For hourglass-shaped cavities the extent of perturbation of a water molecule's behavior from that of bulk solvent is dependent on the position of the water molecule within the cavity.

MATERIALS AND METHODS

MD simulations

MD simulations were performed with CHARMM v. 23f3 (Brooks et al., 1983) run on a DEC2100 computer under VMS/AXP v 6.1. All other calculations were carried out on a Silicon Graphics R4000 Indy. Structure diagrams were drawn using Molscript (Kraulis, 1991). MD simulations used a 1-fs time step, with coordinates saved for analysis every 0.5 ps. After selection from a preequilibrated box of water molecules we heated the system from 0 to 300 K in 6-ps (5 K, 0.1-ps intervals) and equilibrated it for 9 ps at 300 K by rescaling velocities every 0.1 ps. The production stage of the simulation was run for 40 ps. In those simulations that employed velocity rescaling during this stage such rescaling was per-

Received for publication 22 August 1995 and in final form 23 October 1995.

Address reprint requests to Dr. Mark S. P. Sansom, Laboratory of Molecular Biophysics, University of Oxford, The Rex Richards Building, South Parks Road, Oxford OX1 3QU, UK. Tel.: +44-1865-275371; fax: +44-1865-510454; e-mail: mark@biop.ox.ac.uk.

0006-3495/96/02/693/00 $2.00

formed every 0.1 ps. Dynamic properties of water were analyzed over the 80 coordinate set trajectories saved during this latter stage of the simulations. Structural properties were analyzed for the coordinate set generated at the end of the 55-ps total simulation time.

The water model employed was a modified TIP3P three-site model (Jorgensen et al., 1983; Daggett and Levitt, 1993) with partial charges $q_O = -0.834$ and $q_H = +0.417$. The modification permits internal flexibility of the water molecules. Nonbonded interactions (both electrostatic and van der Waals) between distant atoms were truncated by use of a shift function (Brooks et al., 1983) with a cutoff of 13.0 Å.

Cavities

Cavities in which to confine the water molecules were created with the MMFP routine within CHARMM. This allowed cylindrical cavities to be created and required only minor modifications to permit generation of hourglass-shaped cavities. Using MMFP, we created an appropriately shaped potential well such that inside the cavity the potential energy of a water molecule atom was −7.5 kcal/mol relative to outside the cavity. As an atom approaches the wall of the cavity its energy is described by

$$E = \frac{F}{2}\exp\left(-\frac{\Delta}{\lambda}\right) \quad \text{if} \quad \Delta > 0, \tag{1}$$

or by

$$E = F\left[1 - \frac{1}{2}\exp\left(+\frac{\Delta}{\lambda}\right)\right] \quad \text{if} \quad \Delta \le 0, \tag{2}$$

where $F = -7.5$ kcal/mol and $\lambda = 0.25$ Å and in which $\Delta = r - r_{WALL}$, i.e., the distance of the atom from the wall. Note that Eq. 1 applies to atoms *outside* the cavity wall and Eq. 2 applies to atoms *inside* the cavity wall. Thus the cavity walls are purely repulsive (i.e., hydrophobic) and sigmoidal in shape. The walls rise by 90% of their height over a distance of 1.15 Å (as determined by the value of λ). Note that confinement of waters within closed cavities differs from that in channels, which have open ends through which molecules may enter and leave (see Discussion).

Analysis

Three parameters characterizing the dynamic behavior of water molecules were analyzed: the self-diffusion coefficient D and the rotational correlation times τ_1 and τ_2. The self-diffusion coefficient for each water molecule was obtained by evaluation of its mean-square displacement as a function of time:

$$\langle r(t)^2\rangle = \langle (r(t) - r(0))^2\rangle \tag{3}$$

and using the relationship

$$\lim_{t\to\infty} \langle r(t)^2\rangle = 6Dt + \text{constant} \tag{4}$$

to fit the $\langle r(t)^2\rangle$ data for t = 3–6 ps. Inspection of $\langle r(t)^2\rangle$-versus-t curves for individual waters revealed them to approach linearity within this region, justifying the fitting of Eq. 4 to the data. The comparable relationships were used to estimate self-diffusion coefficients parallel to the longitudinal axis of the cavity (D_Z) and in the plane perpendicular to this axis (D_{XY}). Rotational correlation functions were defined in terms of the angle $\theta(t)$ made by the dipole of a water molecule at time t and the dipole of the same water molecule at time *0*. Two rotational correlation functions were estimated for each water molecule:

$$C_1(t) = \langle \cos(\theta(t))\rangle \tag{5}$$

and

$$C_2(t) = \langle (3\cos^2\theta(t) - 1)/2\rangle, \tag{6}$$

which were fitted (for the regions from 0.5 to 5.0 ps) as monoexponential decays with time constants τ_1 and τ_2, respectively. Again, inspection of plots of $C(t)$ for individual waters supported the fitting of monoexponentials to these regions.

Two structural parameters of water within the cavities were analyzed: the water oxygen density profile N_W and the orientation of the water dipole relative to the cavity axes. For a cylinder of length L and radius R the density profile (as a function of the radial coordinate r) is given by

$$N_W(r_i) = \frac{N_i(\Delta r)}{\pi n_W L(r_{i+1}^2 - r_i^2)}. \tag{7}$$

$N_i(\Delta r)$ is the number of water oxygens in a cylindrical shell i of thickness Δr (=0.4 Å) of inner radius r_i and outer radius $r_i + 1$, and n_W is the overall number density of water molecules within the cavity. The orientation of a water molecule dipole relative to a cylindrical cavity is defined by two angles: ϕ is the angle between the dipole μ and the vector -**r** from the oxygen atom to the cavity (z) axis; θ is the angle between μ and z. The distributions of $\cos(\phi)$ and of $\cos(\theta)$ were estimated.

RESULTS

Cylindrical cavities

The first cavity geometry explored was that of a long regular cylinder, providing a first approximation to a transbilayer pore. For example, the pore of the nicotinic acetylcholine receptor (nAChR) is ~40 Å long and ~7 Å in radius (Sansom, unpublished results). That of a bacterial porin (2POR; Weiss and Schulz, 1992) is ~35 Å long and ~7 Å in radius (Sansom and Kerr, 1995). The cylindrical cavities employed in the simulations are defined in Table 1. Thus, for cylinders of length L = 60 Å the radius was varied, and for cylinders of radius R = 6 Å the length was varied, to permit us to explore the influence of cavity geometry on water structure and dynamics.

TABLE 1 Definition of simulations

Simulation	Cavity Geometry	N	R (Å)	L (Å)	Velocity Rescaling?
R3L60_N	CYL	73	3	60	NO
R3L60_R	CYL	73	3	60	YES
R6L15_N	CYL	61	6	15	NO
R6L15_R	CYL	61	6	15	YES
R6L30_N	CYL	144	6	30	NO
R6L30_R	CYL	144	6	30	YES
R6L45_N	CYL	212	6	45	NO
R6L45_R	CYL	212	6	45	YES
R6L60_N	CYL	245	6	60	NO
R6L60_R	CYL	245	6	60	YES
R9L60_N	CYL	498	9	60	NO
R9L60_R	CYL	498	9	60	YES
R12L60_R	CYL	964	12	60	YES
HG1	HG	273	3 to 12	36	YES
HG2	HG	500	3 to 12	60	YES
HG3	HG and PER	490	3 to 12	60	YES

CYL, Cylindrical cavity; HG, hourglass-shaped cavity; PER, periodic boundaries on z; N, number of water molecules; R, cavity radius (minimum and maximum for HG); L, cavity length.

For each geometry two simulations were performed: R*r*L*l*__N in which no velocity rescaling was employed during the final 40 ps of the simulation and R*r*L*l*__R in which velocity rescaling was employed (*r* designates the radius of the cylinder, *l* its length; see Table 1 for details). For the smallest cavities (simulations R3L60__N and R6L15__N) it was found that in the absence of velocity rescaling the temperature drifted downward. For the larger cavities no significant difference in mean temperature was observed between those simulations without velocity rescaling and those with.

For comparison with the cavity simulations, we simulated a box of 231 water molecules, dimensions (19.042 × 19.042 × 19.042) Å^3, using periodic boundaries. This was analyzed in exactly the same fashion as the cavity-confined waters to yield estimates of the dynamic parameters of modified TIP3P solvent in the "bulk" state. The self-diffusion coefficient thus obtained, $D = 0.32$ Å^2 ps^{-1}, is slightly less than that for unmodified TIP3P ($D = 0.40$ Å^2 ps^{-1}; Daggett and Levitt, 1993) and therefore is somewhat closer to the experimental value for water at 300 K ($D = 0.23$ Å^2 ps^{-1}; Eisenberg and Kauzmann, 1969).

Snapshots of the structures of R3L60__R, R6L60__R, R9L60__R, and R12L60__R at the end of these simulations are shown in Fig. 1, viewed down the pore (*z*) axis. It is evident that in all four simulations the disposition of the water molecules within the cylinder is nonrandom. This is clearest for R3L60__R and is less evidently so for R12L60__R. R3L60__R is something of a special case: in this rather narrow cylinder the water molecules are highly ordered to form four H-bonded "strands" of molecules running parallel to the cavity axis. This was particularly evident in simulation R3L60__N, in which ordering of the water was so pronounced that the temperature of the system dropped by ~25 K within 40 ps. Although simulations with wider cylinders did not yield such "strands" of water molecules, from examination of Fig. 1 it can be seen that the water molecules are clustered into concentric shells. In each simulation the outermost shell is the most prominent. This may be compared with ordering observed in simulations of water molecules between two planar surfaces (Jonsson, 1981; Marchesi, 1983; Barabino et al., 1984; Lee et al., 1984; Rossky and Lee, 1989) or within spherical hydrophobic cavities (Belch and Berkowitz, 1985; Zhang et al., 1995).

The presence of concentric cylindrical shells of water molecules was confirmed by estimation of water oxygen density profiles (see Fig. 2). In these profiles the water density N_W is shown as a function of the distance from the cavity wall, i.e., $R - r$. The profile for R6L60__R reveals quite clearly that two distinct shells of water molecules are formed. The R12L60__R profile suggests that even for a higher radius the shell structure is preserved, with the shells becoming less distinct as one moves away from the cavity wall (i.e., as $R - r$ increases).

Examination of the snapshots of water structure suggests that there is a preferential orientation of the water molecules

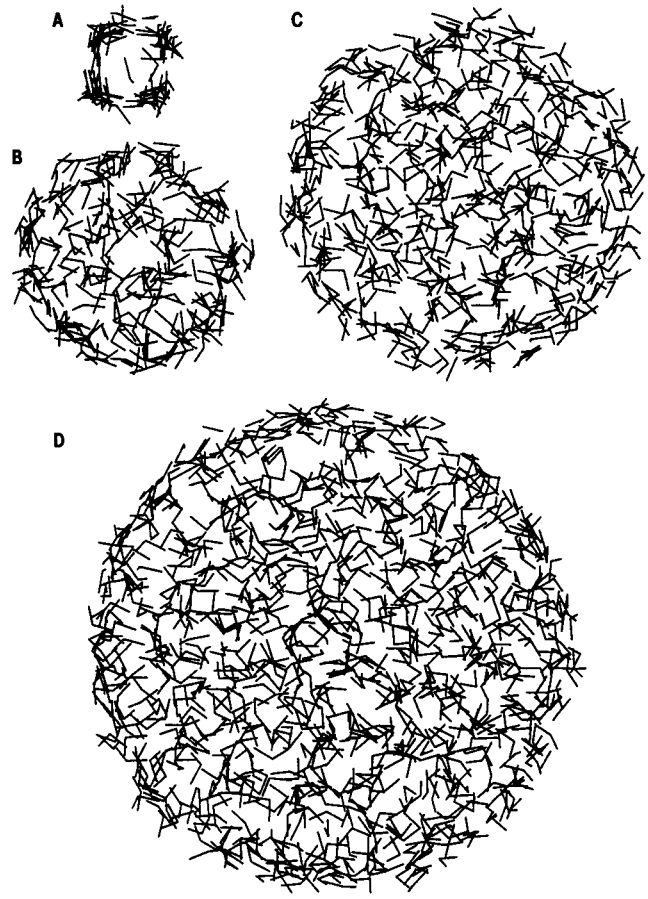

FIGURE 1Water in cylindrical cavities. Views down *z* of water structure at the ends of simulations (*A*) R3L60__R, (*B*) R6L60__R, (*C*) R9L60__R, (*D*) R12L60__R. The concentric shells of water yielded by these simulations are visible.

in the outermost shell of each simulation. We tested this probability by estimating the distributions of cos(ϕ) and of cos(θ) for the outermost shell (defined as those water molecules for which $0 < R - r < 3$ Å; Fig. 3). For all four simulations the distribution of cos(ϕ) peaks at $\phi \sim 90°$ and that of cos(θ) at $\theta \sim 0°$ and 180°. Thus in the outer shell the waters are preferentially oriented relative to the cylinder axes (see below and Fig. 6 below). Repeating the analysis for the inner shells suggests that this orientation effect does not extend significantly beyond the outermost shell.

The dynamic behavior of water within the cylindrical cavities was examined in terms of translational mobility (self-diffusion coefficient *D*) and of rotational mobility (rotational reorientation rates, τ_1^{-1} and τ_2^{-1}; Table 2). Comparison of simulations R3L60, R6L60, R9L60, and R12L60 suggests that the self-diffusion coefficient of water molecules is reduced relative to the bulk solvent for $R = 3$ and $R = 6$ Å cylinders but approaches that of bulk water for $R = 9$ and $R = 12$ Å. Separate analysis of the components of the self-diffusion coefficients parallel to (D_Z) and perpendicular to (D_{XY}), the cavity axis, suggests that the latter is generally somewhat smaller. However, the difference is

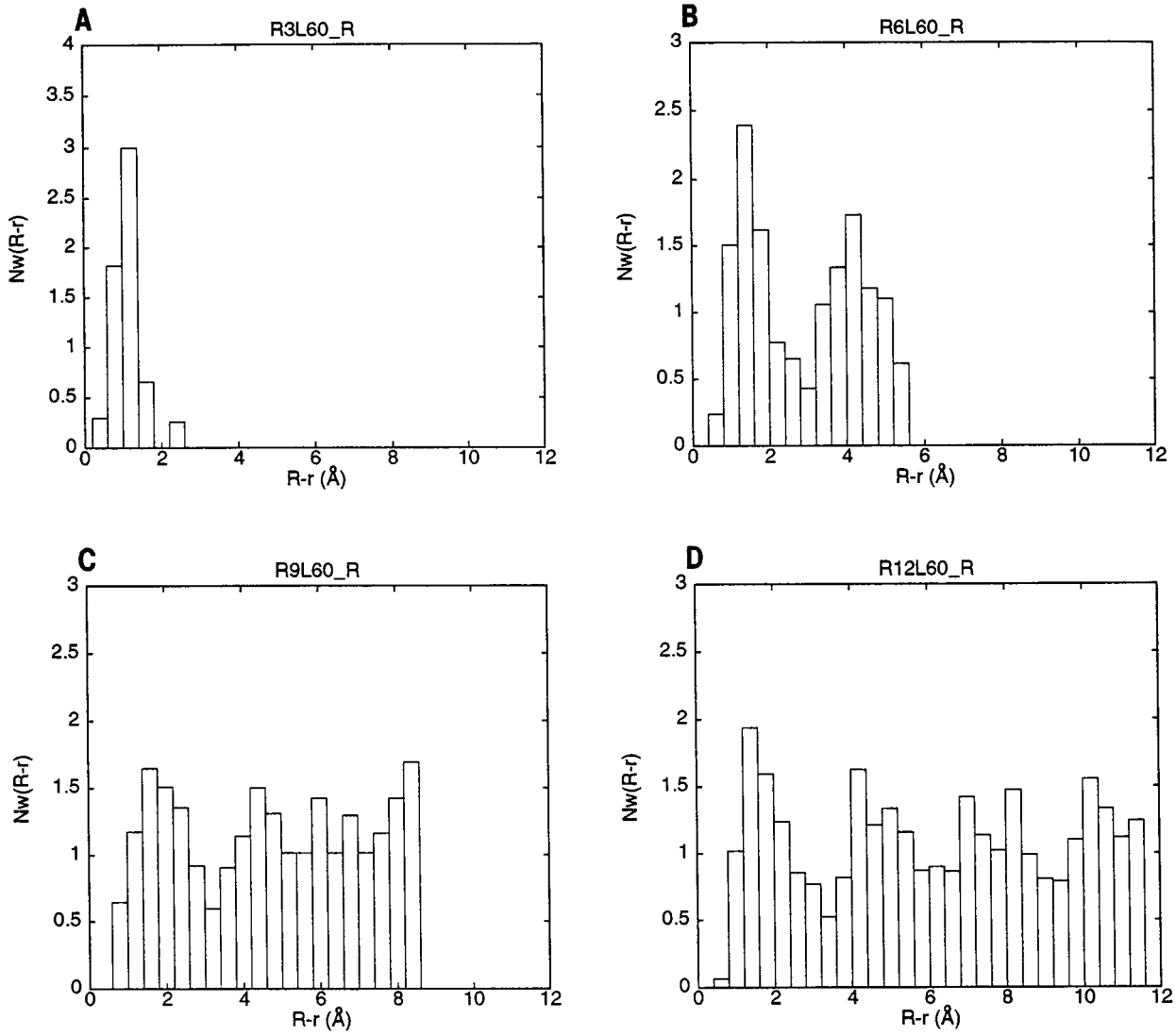

FIGURE 2 Water density profiles. The normalized density $N_W(R - r)$ of water as a function of the distance from the cavity wall, $R - r$, is shown for simulations (*A*) R3L60__R, (*B*) R6L60__R, (*C*) R9L60__R, (*D*) R12L60__R. Peaks in the profiles correspond to the concentric shells of water molecules in Fig. 1.

not statistically significant. Some perturbation of rotational mobility (particularly τ_2^{-1}) may persist even to $R = 9$ Å. The value of τ_2^{-1} for $R = 3$ Å is approximately a third of that for "bulk" water. The degree of immobilization of water molecules is also dependent on the length of the cylindrical cavity. Comparing simulations R6L15, R6L30, R6L45, and R6L60 reveals an increase in mobility as L is increased from 15 to 60 Å.

The water molecules may switch between the concentric shells within the cylindrical cavities, but the dynamics of switching varies with the overall cavity radius and between different shells within the same cavity (Table 3). Thus, in each case the mean residence time is longest within the outermost shell, typically approximately twice that for inner shells. Furthermore, the mean residence time for the outer shell falls as the overall cavity radius increases. For the wider (e.g., R9L60 and R12L60) cavities, the residence time within the (poorly defined) inner shells is ~3 ps, whereas for the outermost shell it is ~6 ps. These differences in mean residence times parallel the degree of definition of the shells (Fig. 2) for different cavity radii.

Comparison of simulations without and with velocity rescaling suggests that in narrow pores ($R = 3$ and $R = 6$ Å) in the absence of velocity rescaling the water molecules become highly ordered as the temperature of the system falls. For the higher-radius cavities the presence or absence of velocity rescaling has no significant effects on the water dynamic behavior. Thus, for comparisons and further simulations velocity rescaling has been employed.

Hourglass-shaped cavities

Several transbilayer pores do not have the same radius throughout their length. For example, both the nAChR and

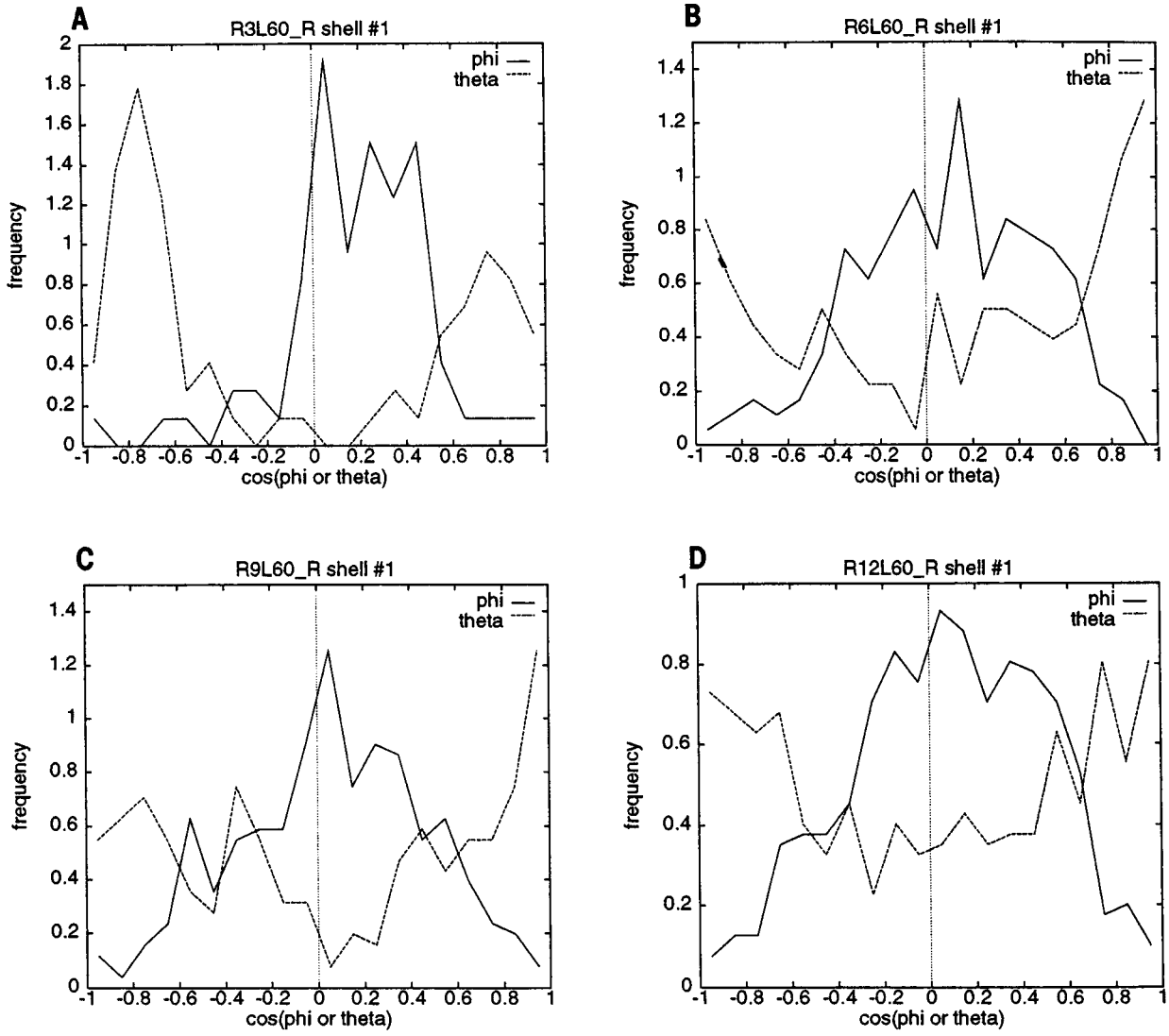

FIGURE 3 Dipole angle distribution functions: ϕ is the angle between the water dipole and the normal to the cavity wall; θ is the angle between the water dipole and the cavity (z) axis. The distributions of $\cos(\phi)$ and of $\cos(\theta)$ are shown for the outermost shell of waters for simulations (*A*) R3L60__R, (*B*) R6L60__R, (*C*) R9L60__R, (*D*) R12L60__R.

2POR pores have central constrictions. One might therefore anticipate that the dynamic behavior of water molecules within such pores would vary with the position of the water along the pore (z) axis. To investigate this we have simulated the properties of water molecules in hourglass-shaped cavities (Fig. 4 and Table 4). In these simulations the radius of the central narrow region of the pore was set to 3 Å and that of the mouths of the pore to 12 Å. Thus a single cavity spans the range of radii studied in the previous simulations. The cavity length was varied between simulations HG1 and HG2. In both simulations velocity rescaling was applied. Furthermore, to study the effects of removing the end walls of the cavities, in simulation HG3 we applied periodic boundaries (on z only) such that no restrictions were placed on the movement of water molecules in/out of the mouths of the channel.

To analyze possible dependence of water dynamics on z we divided each cavity into a central narrow zone ($z <$ 7.5 Å) and two mouth regions ($z >$ 7.5 Å; see Table 4). Water molecules were assigned to a zone on the basis of their average z coordinates over the last 40 ps of the simulation. This is expected to lead to some "blurring" of effects, as a water molecule may cross between zones during the duration of the simulation. From Table 4 it is evident that, in all three HG simulations, self-diffusion coefficients and rotational reorientation rates are consistently higher for the mouth zones than for the central zone of the pore. The difference between the zones is small, partly as a consequence of the blurring effect. That water dynamic parameters vary significantly with z is evident if one plots these parameters as a function of the mean z coordinate of water molecules (e.g., for HG2 in Fig. 5abc). From such graphs it

TABLE 2 Cylindrical cavities: water properties

Simulation	T (K)	D (Å^2 ps^{-1})	D_{XY} (Å^2 ps^{-1})	D_Z (Å^2 ps^{-1})	τ_1^{-1} (ps^{-1})	τ_2^{-1} (ps^{-1})
Experimental	300	0.23 [1]	–	–	0.21 [1]	0.52 [2]
"Bulk"	302 (8)	0.32 (0.12)	–	–	0.30 (0.16)	0.64 (0.28)
R3L60_N	288 (14)	0.06 (0.05)	0.06 (0.05)	0.06 (0.05)	0.12 (0.13)	0.23 (0.18)
R3L60_R	301 (13)	0.15 (0.05)	0.18 (0.08)	0.08 (0.09)	0.10 (0.07)	0.22 (0.11)
R6L15_N	275 (14)	0.07 (0.04)	0.07 (0.04)	0.08 (0.07)	0.14 (0.12)	0.24 (0.14)
R6L15_R	300 (15)	0.15 (0.07)	0.17 (0.09)	0.12 (0.11)	0.13 (0.12)	0.29 (0.24)
R6L30_N	296 (10)	0.08 (0.06)	0.07 (0.07)	0.10 (0.09)	0.15 (0.13)	0.29 (0.21)
R6L30_R	300 (10)	0.13 (0.07)	0.13 (0.07)	0.13 (0.12)	0.16 (0.16)	0.31 (0.21)
R6L45_N	286 (8)	0.10 (0.06)	0.10 (0.08)	0.11 (0.09)	0.13 (0.11)	0.26 (0.18)
R6L45_R	299 (8)	0.17 (0.08)	0.18 (0.11)	0.15 (0.12)	0.17 (0.13)	0.37 (0.26)
R6L60_N	295 (8)	0.19 (0.10)	0.17 (0.10)	0.24 (0.20)	0.20 (0.16)	0.38 (0.25)
R6L60_R	299 (7)	0.27 (0.14)	0.30 (0.17)	0.21 (0.18)	0.20 (0.14)	0.41 (0.27)
R9L60_N	301 (5)	0.31 (0.14)	0.30 (0.18)	0.31 (0.22)	0.27 (0.18)	0.56 (0.33)
R9L60_R	300 (5)	0.27 (0.14)	0.26 (0.15)	0.29 (0.25)	0.26 (0.16)	0.52 (0.30)
R12L60_R	296 (3)	0.28 (0.13)	0.27 (0.16)	0.30 (0.23)	0.26 (0.18)	0.55 (0.33)

The "bulk" simulation was for a (19.042 × 19.042 × 19.042) Å^3 box of water, using periodic boundaries. All simulations were run for 55 ps = 6 ps (heating) + 9 ps (equilibration) + 40 ps (production). Water properties were analyzed for the last 40 ps. T is the average temperature; D is the self-diffusion coefficient; D_{XY} and D_Z are the self-diffusion coefficients in the xy plane (i.e., perpendicular to the cavity axis) and along z (i.e., parallel to the cavity axis); τ_1^{-1} and τ_2^{-1} are the reciprocals of the first- and second-order rotational correlation times. All values are given as means (SD) for all water molecules in the cavity. [1], Eisenberg and Kauzmann (1969); [2], Rahman and Stillinger (1971).

is clear that the mobility of water molecules is lowest in the narrow central region of the cavity. This pattern is preserved when periodic boundary conditions are applied during the simulation, demonstrating that the pattern is not an artifact of the end walls of the cavity.

In addition to the gradient of mobility within hourglass-shaped cavities, orientational effects on water molecules of the outermost shell are similar to those seen in cylindrical cavities (Fig. 5 *D*). Thus a cavity whose shape is a realistic approximation to that of a biological pore exhibits both preferred orientations and reduced mobility of the water molecules within them.

TABLE 3 Water residence times in shells

Simulation	Shell Number	Radius (Å)	$\langle t \rangle$ (ps)
R6L60_N	1	0–3	5.1 (8.2)
	2	3–6	11.5 (12.4)
R6L60_R	1	0–3	4.8 (8.1)
	2	3–6	10.8 (11.8)
R9L60_N	1	0–3	2.9 (4.0)
	2	3–6	3.0 (4.2)
	3	6–9	5.8 (7.0)
R9L60_R	1	0–3	3.0 (4.4)
	2	3–6	3.1 (4.1)
	3	6–9	6.1 (7.6)
R12L60_R	1	0–3	3.1 (4.3)
	2	3–6	3.1 (3.9)
	3	6–9	3.3 (4.7)
	4	9–12	6.9 (8.2)

Concentric cylindrical shells within each cavity are defined on the basis of the analysis presented in Fig. 2. For each shell the mean residence time (SD), $\langle t \rangle$, is given.

DISCUSSION

Limitations of the simulations

Before considering the implications of the results one should analyze possible limitations of the simulations. The first consideration is of the potential function used to form the cavities in which the waters were confined. The function employed is purely repulsive and results in a rigid cavity wall. We chose this function so we could focus on effects of confinement per se, without including any dispersive interactions of water molecules with the wall of a hydrophobic cavity. This contrasts with the conditions for some other studies (Barabino et al., 1984; Lee et al., 1984; Zhang et al., 1995) in which an L-J potential is used to generate walls within which water molecules are confined. A major difference between our channel-like cavities and a protein channel is that the wall of the simple cavity is rigid, whereas in a water–protein system collisions of waters with the wall may be inelastic. Finally, in considering hydrophobic cavities, it may be appropriate to include an image-charge effect to model the low dielectric nature of the wall-forming medium (Barabino et al., 1984). Again, as we wished in these initial studies to focus on the effects of confinement, we did not include such electrostatic interactions.

Four other possible limitations of our simulations should be considered: a) the duration of the simulations, b) the effects of employing closed cavities, c) the water model used, and d) the water density within the cavities. The duration (55 ps total) of the MD simulations is relatively short, a compromise that enabled multiple simulations to be carried out. Analysis of 100-ps simulations for some of the systems suggested that no significant changes in dynamic

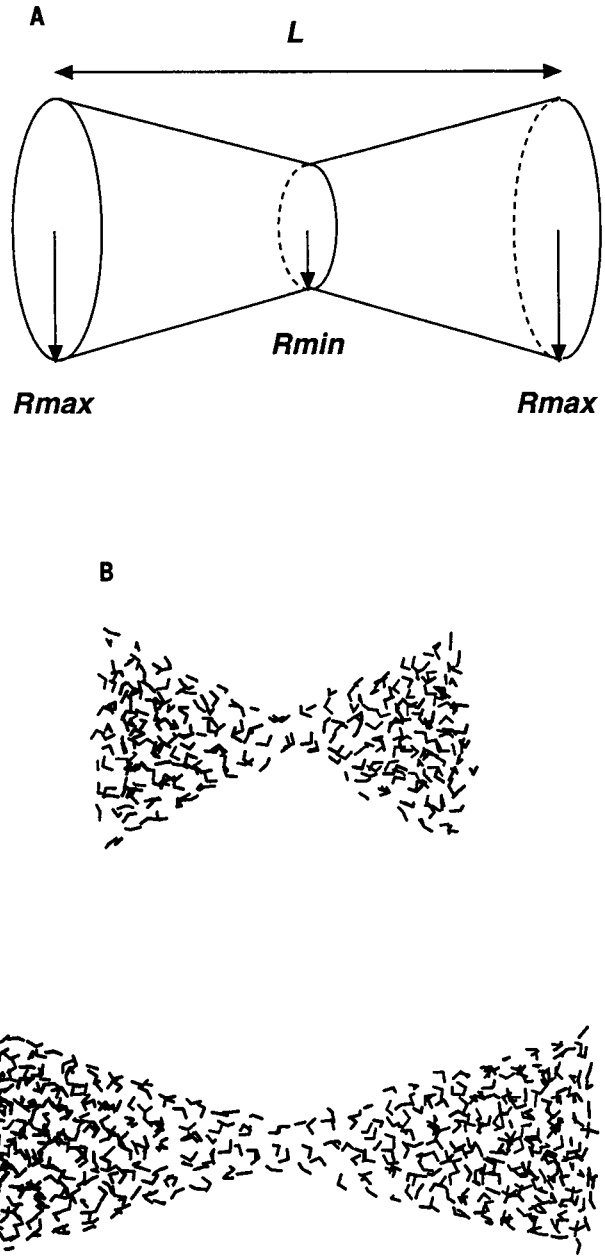

FIGURE 4 Hourglass-shaped cavities. *A* is a schematic diagram of the cavity shape. *B* and *C* show the water structures at the ends of simulations HG1 and HG2, respectively.

and structural parameters occurred, although the standard deviations of the estimates were lower.

The effects of using closed cavities have been addressed in two sets of simulations: the R6 simulations in which L was varied and the use of periodic boundaries on z for HG2. In both cases the results suggest that, provided the cavity is sufficiently long, the presence of boundaries at the ends of the cavity does not alter the dynamic behavior of most of the water molecules. This is also evident from plots of, e.g., D versus z for $L = 60$ Å cylindrical cavities (not shown).

The modified TIP3P water molecule was chosen to be compatible with simulations of protein channel/water systems carried out with CHARMM. Although improved water models have been described (Daggett and Levitt, 1993), the modified TIP3P model has been quite widely used in simulations of protein–water systems. Other studies (Daggett and Levitt, 1993), plus our own control results, suggest that the TIP3P model overestimates both D and the rotational reorientation rates. However, as our comparisons are of different cavity geometries with the bulk simulation rather than of absolute values of parameters, this does not present too great a difficulty in interpreting the results.

TABLE 4 Hourglass-shaped cavities: water properties

Simulation	Zone	N	D (Å^2 ps^{-1})	τ_1^{-1} (ps^{-1})	τ_2^{-1} (ps^{-1})
HG1	$z < -7.5$	114	0.22 (0.11)	0.19 (0.15)	0.37 (0.29)
	$\|z\| < 7.5$	41	0.16 (0.08)	0.17 (0.13)	0.32 (0.19)
	$z > +7.5$	118	0.18 (0.08)	0.19 (0.13)	0.33 (0.20)
HG2	$z < -7.5$	233	0.18 (0.08)	0.20 (0.16)	0.44 (0.33)
	$\|z\| < 7.5$	34	0.12 (0.04)	0.14 (0.12)	0.24 (0.15)
	$z > +7.5$	233	0.18 (0.08)	0.19 (0.16)	0.38 (0.27)
HG3	$z < -7.5$	224	0.21 (0.10)	0.24 (0.19)	0.52 (0.35)
	$\|z\| < 7.5$	31	0.16 (0.07)	0.19 (0.14)	0.38 (0.28)
	$z > +7.5$	235	0.20 (0.10)	0.27 (0.20)	0.53 (0.36)

The water densities within the cavities were also considered as a possible source of variations in D. The densities differed slightly in some cases from bulk density (e.g., particularly for R3L60). It is well known that the dynamics of a liquid depends on the liquid's density. In simple van der Waals liquids a decrease in density leads to an increase in diffusion constant (Cohen and Turnbull, 1959). Water near 300 K shows anomalous behavior (Sciortino et al., 1992; Vaisman et al., 1993), with an decrease in density ("stretched water") resulting in a decrease in D. At higher temperatures water behaves as a simple liquid. However, comparison of the differences in water density from the bulk for the cavities reveals no correlation with the deviations in D from the bulk value. Even more convincingly, for simulation HG2, e.g., which shows a gradient in D along the cavity axis (Fig. 5 *A*), the density does *not* vary along the same axis. Thus, the perturbation of cavity dynamics from that of the bulk does not seem to be a density effect.

Comparison with other studies

There have been several simulation studies of water within confined geometries (Jonsson, 1981; Marchesi, 1983; Barabino et al., 1984; Lee et al., 1984; Belch and Berkowitz, 1985; Rossky and Lee, 1989; Zhang et al., 1995), but few if any of channel-like cavities. Granick (1991) provides an extensive review of both experimental and computational studies of confined liquids, with a general conclusion that relaxation times are prolonged by confinement in volumes of molecular dimensions. Simulations of water molecules between two planar walls (Jonsson, 1981; Marchesi, 1983; Barabino et al., 1984; Lee et al., 1984) demonstrate preferential ordering of water molecules near the wall such that

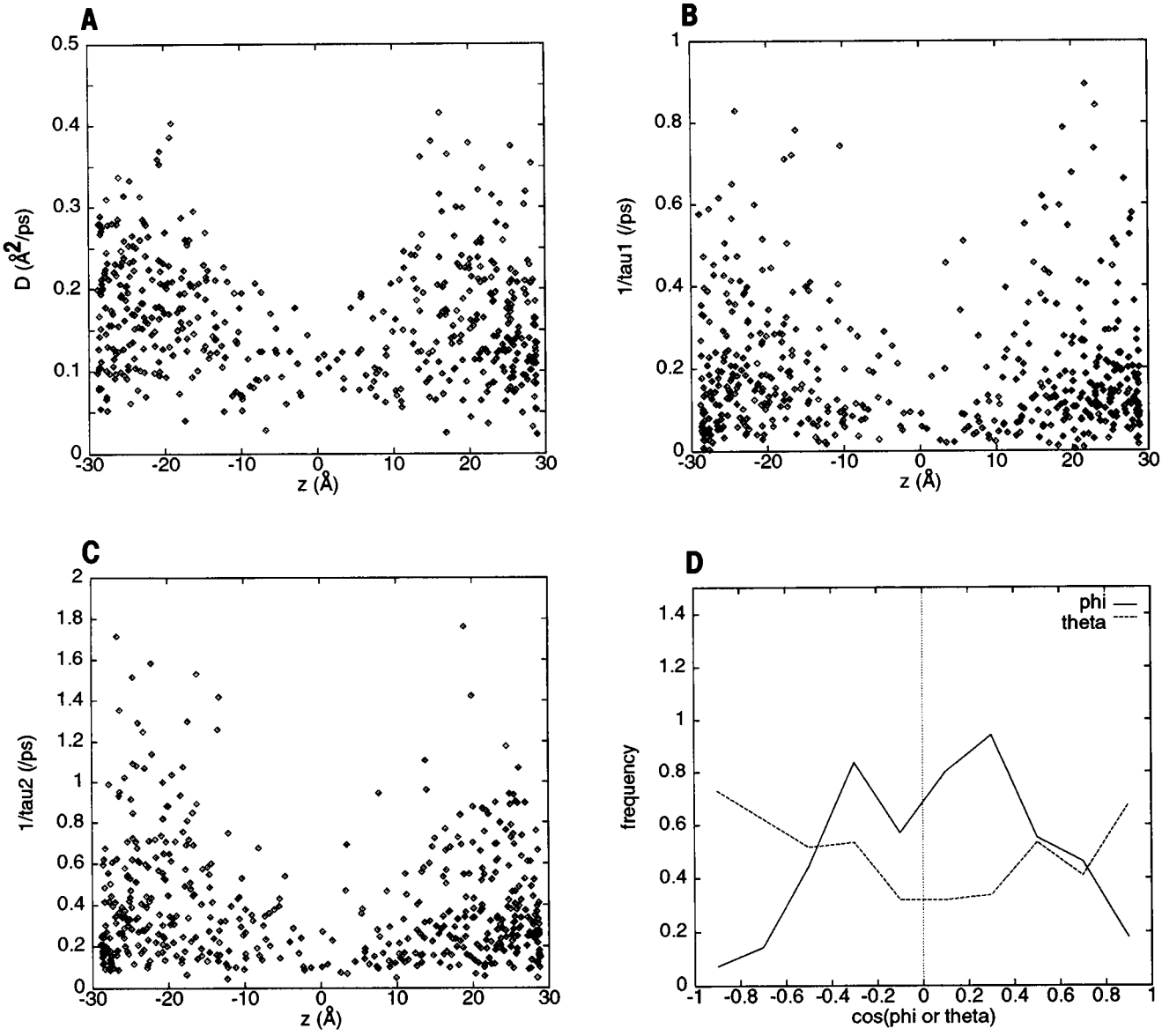

FIGURE 5 Dynamics of water within an hourglass-shaped cavity. Three parameters characterizing the dynamic behavior of water molecules in simulation HG2 are shown as a function of the average z coordinate of the water molecule: (*A*) D, (*B*) τ_1^{-1}, (*C*) τ_2^{-1}. In each case a progressive immobilization of the water molecules toward the center of the cavity ($z = 0$) is evident. *D* shows the dipole angle distribution functions for simulation HG2.

water dipoles prefer to be approximately perpendicular to the wall normal. Marchesi (1983), using a rigid wall, also demonstrated a reduction in D and in τ_1^{-1} for waters adjacent to the wall. Belch and Berkowitz (1985) and Zhang et al. (1995) have simulated waters confined within spherical cavities. In both cases, preferential ordering of the wall-adjacent waters with their dipoles approximately perpendicular to the wall normal was observed. Thus, our simulation results are in general agreement with previous simulations concerning the ordering and preferential orientation of wall-adjacent waters. This agreement among a number of studies, which used different water models and different wall potentials, is encouraging, as it suggests that the results concerning water orientation are relatively robust to simulation details. Somewhat more perplexing is the observation of Zhang et al. (1995) that D is *increased* for cavity-confined water relative to bulk water. This contrasts with our results and suggests that dynamic properties may be rather more sensitive to the details of simulation procedures. The results of Barabino et al. (1984) also suggested that dynamic properties varied with simulation conditions, although in all cases the latter study revealed a *decrease* in D for wall-adjacent relative to bulk water. In this context one should remember the general conclusion of Granick (1991) that confinement of liquids tends to slow their relaxation.

Biological relevance

In these studies we have focused on the effects of confinement on water structure and dynamics with channel-shaped

cavities. It should be remembered that protein channels present intrapore waters with a complex spatial and electrostatic environment in addition to confining them within a volume of molecular dimensions. Furthermore, protein channels have flexible walls. Thus one might anticipate more complex perturbations of water structure and dynamics, possibly as a function of the position of a water molecule within the protein channel (Breed et al., 1996). The results of the current studies are of value in that they help us to dissect out the interactions taking place in more complex channel systems. An understanding of the behavior of water molecules within channels is a necessary prerequisite to a molecular description of the properties of ion channels (Chiu et al., 1991, 1993), and our results contribute to such an understanding.

Our results show that ordering and preferential orientation of water molecules occur within even simple models of transbilayer pores. As illustrated in Fig. 6*A*, the preferred orientation of wall-adjacent water molecules is such that the molecular dipole is approximately parallel (or antiparallel) to the pore axis. However, the *z*-axis projections of the water dipoles are randomly distributed, showing that the waters confined within the cavities do not align to form "dipolar wires." This is the case independently of whether velocity scaling is applied. Simulations on water molecules within protein pores (Breed et al., 1996) suggest that further orientational effects that form dipolar wires may occur as a result of electrostatic interactions between water molecules and the protein. The second effect evident from the simple models is that translational and rotational relaxation rates decrease when water molecules are confined within narrow pores. This has already been observed in the extreme case of a single file of water molecules within the gramicidin A pore (Chiu et al., 1991, 1993). Our simulations suggest that a reduction in rotational relaxation rates may still occur in somewhat wider channels, of up to 6-Å radius. Furthermore, in more complex channel geometries spatial gradients of rotational relaxation rates may be found (Fig. 6 *b*).

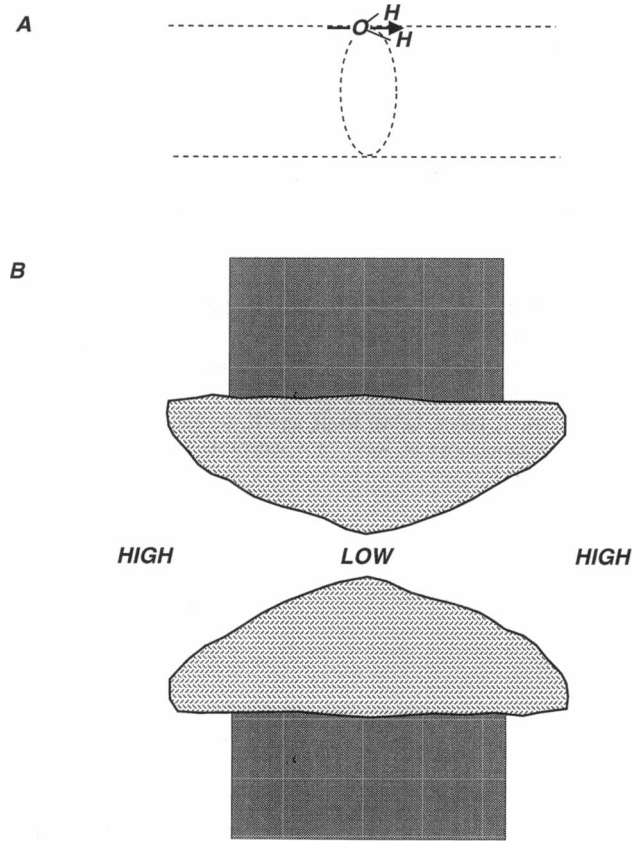

FIGURE 6 (*A*) Preferred orientation of a molecule in the first shell of waters in a cylindrical pore. The dipole moment is shown oriented such that $\phi = 90°$ and $\theta = 0°$. (*B*) Schematic diagram of a transbilayer pore showing the regions expected to exhibit high (i.e., bulk) and low solvent mobility.

Perturbation of solvent properties from those in bulk water is of importance with respect to continuum electrostatics calculations on transbilayer pores (Karshikoff et al., 1994). Reduction of rotational relaxation rates of water molecules within narrow regions of pores suggests that the effective dielectric constant within such regions is less than that of bulk water ($\epsilon = 80$). Problems remain of to what extent ϵ is reduced and also of how to develop a theoretical and computational framework to handle spatial gradients of ϵ within pores. To take one example, simulation HG2, corresponding to a pore of minimum radius 3 Å, revealed markedly slower water motions in the narrowest region of the pore (Fig. 5). Current models of the closed conformation of the nAChR (Unwin, 1993; Sansom et al., 1995) suggest that a ring of channel-occluding leucine residues form a constricted hydrophobic zone of radius ~2 Å. Any water molecules in the vicinity of this ring are expected to have dynamic properties significantly different from those of bulk water. One may speculate as to the importance of this in maintaining the low conductance of the closed form of the channel.

An investigation of the effects of confinement on water structure and dynamics is only the beginning of an analysis of the properties of water within ion channels. A number of more realistic simulations of solvated channels are required, as have already been performed for gramicidin (Chiu et al., 1991, 1993), to complete the picture. Studies on a number of channel models, both α-helix bundles and β-barrels, suggest that the perturbations of water dynamics and structure as observed in the current study may be somewhat greater once protein–water electrostatic interactions are taken into account (Breed et al., 1996). We are now applying simulations of intrapore water to models of the open and closed conformations of the nAChR transbilayer pore (Sansom, 1995; Unwin, 1995) and to models of channels formed by amphipathic α-helical peptides (Lear et al., 1988; Kerr et al., 1994).

This work was supported by grants from the Wellcome Trust. J.B. is an MRC research student. Our thanks to the Oxford Centre for Molecular Science for computational facilities. Our thanks to Peter Jordan (Brandeis) for his helpful comments and interest in this work.

REFERENCES

Barabino, G., C. Gavotti, and M. Marchesi. 1984. Molecular dynamics simulation of water near walls using an improved wall-water interaction potential. *Chem. Phys. Lett.* 104:478–484.

Belch, A. C., and M. Berkowitz. 1985. Molecular dynamics simulations of TIPS2 water restricted by a spherical hydrophobic boundary. *Chem. Phys. Lett.* 113:278–282.

Breed, J., R. Sankararamakrishnan, I. D. Kerr, and M. S. P. Sansom. 1996. Molecular dynamics simulations of water within models of transbilayer pores. *Biophys. J.* In press.

Brooks, B. R., R. E. Bruccoleri, B. D. Olafson, D. J. States, S. Swaminathan, and M. Karplus. 1983. CHARMM: a program for macromolecular energy, minimisation, and dynamics calculations. *J. Comp. Chem.* 4:187–217.

Chiu, S. W., E. Jakobsson, S. Subramanian, and J. A. McCammon. 1991. Time-correlation analysis of simulated water motion in flexible and rigid gramicidin channels. *Biophys. J.* 60:273–285.

Chiu, S. W., J. A. Novotny, and E. Jakobsson. 1993. The nature of ion and water barrier crossings in a simulated ion channel. *Biophys. J.* 64: 98–109.

Cohen, M. H., and D. Turnbull. 1959. Molecular transport in liquids and gases. *J. Chem. Phys.* 31:1164–1169.

Cowan, S. W., T. Schirmer, G. Rummel, M. Steiert, R. Ghosh, R. A. Pauptit, J. N. Jansonius, and J. P. Rosenbusch. 1992. Crystal structures explain functional properties of two *E. coli* porins. *Nature (London).* 358:727–733.

Daggett, V., and M. Levitt. 1993. Realistic simulations of native-protein dynamics in solution and beyond. *Annu. Rev. Biophys. Biomol. Struct.* 22:353–380.

Dani, J. A., and D. G. Levitt. 1990. Diffusion and kinetic approaches to describe permeation in ionic channels. *J. Theor. Biol.* 146:289–301.

Eisenberg, D., and W. Kauzmann. 1969. The Structure and Properties of Water. Oxford University Press, Oxford.

Engel, A., T. Walz, and P. Agre. 1994. The aquaporin family of membrane water channels. *Curr. Opin. Struct. Biol.* 4:545–553.

Granick, S. 1991. Motions and relaxations of confined liquids. *Science.* 253:1374–1379.

Green, M. E., and J. Lu. 1995. Monte-Carlo simulations of the effects of charges on water and ions in a tapered pore. *J. Coll. Interface Sci.* 171:117–126.

Hille, B. 1992. Ionic Channels of Excitable Membranes, 2nd ed. Sinauer Associates, Inc., Sunderland, MA.

Jonsson, B. 1981. Monte Carlo simulations of liquid water between two rigid walls. *Chem. Phys. Lett.* 82:520–525.

Jorgensen, W. L., J. Chandresekhar, J. D. Madura, R. W. Impey, and M. L. Klein. 1983. Comparison of simple potential functions for simulating liquid water. *J. Chem. Phys.* 79:926–935.

Karshikoff, A., V. Spassov, S. W. Cowan, R. Ladenstein, and T. Schirmer. 1994. Electrostatic properties of two porin channels from *Escherichia coli*. *J. Mol. Biol.* 240:372–384.

Kerr, I. D., R. Sankararamakrishnan, O. S. Smart, and M. S. P. Sansom. 1994. Parallel helix bundles and ion channels: molecular modeling via simulated annealing and restrained molecular dynamics. *Biophys. J.* 67:1501–1515.

Kraulis, P. J. 1991. MOLSCRIPT: a program to produce both detailed and schematic plots of protein structures. *J. Appl. Cryst.* 24:946–950.

Kreusch, A., and G. E. Schulz. 1994. Refined structure of the porin from *Rhodobacter blastica*. *J. Mol. Biol.* 243:891–905.

Lear, J. D., Z. R. Wasserman, and W. F. DeGrado. 1988. Synthetic amphiphilic peptide models for protein ion channels. *Science* 240: 1177–1181.

Lee, C. Y., J. A. McCammon, and P. J. Rossky. 1984. The structure of liquid water at an extended hydrophobic surface. *J. Chem. Phys.* 80: 4448–4455.

Marchesi, M. 1983. Molecular dynamics simulation of liquid water between two walls. *Chem. Phys. Lett.* 97:224–230.

Rahman, A., and F. H. Stillinger. 1971. Molecular dynamics study of liquid water. *J. Chem. Phys.* 55:3336–3359.

Rossky, P. J., and S. H. Lee. 1989. Structure and dynamics of water at interfaces. *Chem. Scr.* 29A:93–95.

Sancho, M., M. B. Partenskii, V. Dorman, and P. C. Jordan. 1995. Extended dipolar chain model for ion channels: electrostriction effects and the translocational energy barrier. *Biophys. J.* 68:427–433.

Sansom, M. S. P. 1995. Twist to open. *Curr. Biol.* 5:373–375.

Sansom, M. S. P., and I. D. Kerr. 1995. Transbilayer pores formed by β-barrels: molecular modeling of pore structures and properties. *Biophys. J.* 69:1334–1343.

Sansom, M. S. P., R. Sankararamakrishnan, and I. D. Kerr. 1995. Modelling membrane proteins using structural restraints. *Nature Struct. Biol.* 2:624–631.

Sciortino, F., A. Geiger, and H. E. Stanley. 1992. Network defects and molecular mobility in liquid water. *J. Chem. Phys.* 96:3857–3865.

Teeter, M. M. 1991. Water protein interactions: theory and experiment. *Ann. Rev. Biophys. Biophys. Chem.* 20:577–600.

Unwin, N. 1989. The structure of ion channels in membranes of excitable cells. *Neuron.* 3:665–676.

Unwin, N. 1993. Nicotinic acetylcholine receptor at 9 Å resolution. *J. Mol. Biol.* 229:1101–1124.

Unwin, N. 1995. Acetylcholine receptor channel imaged in the open state. *Nature (London).* 373:37–43.

Vaisman, I. I., L. Perara, and M. L. Berkowitz. 1993. Mobility of stretched water. *J. Chem. Phys.* 9:9859–9862.

Weiss, M. S., and G. E. Schulz. 1992. Structure of porin refined at 1.8A resolution. *J. Mol. Biol.* 227:493–509.

Zhang, L., H. T. Davis, D. M. Kroll, and H. S. White. 1995. Molecular dynamics simulations of water in a spherical cavity. *J. Phys. Chem.* 99:2878–2884.